



ION-INDUCED SECONDARY ELECTRON EMISSION FROM ^{58}Ni AND ^{60}Ni : EVIDENCE OF SECONDARY ELECTRONS GENERATED BY THE RECOILING TARGET ATOMS

SHAKIR ULLAH, A.H. DOGAR and *A. QAYYUM

Physics Division, Directorate of Science, PINSTECH, P.O. Nilore, Islamabad, Pakistan

(Received May 28, 2010 and accepted in revised form June 14, 2010)

We have measured the secondary electron yield of clean ^{58}Ni and ^{60}Ni bombarded with 2-10 keV Ar^+ ions. It was found that secondary electron yield of ^{58}Ni is consistently high as compared to the ^{60}Ni . This result is not in line with the most theoretical model of kinetic electron emission, which predict strict proportionality between secondary electron yield and electronic stopping power. We have demonstrated that the measured secondary electron yield is also related to the nuclear stopping power. We thus conclude that higher secondary electron yield of ^{58}Ni is due to the larger contribution of the recoiling target atoms to the secondary electron yield.

PACS: 34.50.Dy; 79.20.Rf

Keywords: Ion-induced electron emission, Nuclear stopping, Isotope effect, Ni

1. Introduction

Secondary electron emission induced by impact of fast projectile ions on the solid surface is of genuine interest in fundamental research and plays an important role in many technological applications, for example, in precise measurement of ion currents, in particle detection, in surface analysis techniques and in plasma wall interactions [1,2]. Two production mechanisms have been visualized for secondary electron emission, namely kinetic and potential emission. The kinetic electron emission (KEE) results from the atomic excitations in the target by transfer of kinetic energy from incident projectile ions. One of the most important quantities to describe KEE is the mean number of emitted electrons per incident ion, the kinetic electron yield γ . The knowledge of γ provides important information about the basic interaction mechanism of projectile ions with atoms and electrons in the solid. It is common to nearly all-theoretical approaches that the electronic excitation leading to KEE from material surface involves a complex scenario, which consist of primary excitation processes, the subsequent electron transport to the surface, and finally the escape of electrons through the surface into vacuum. Most KEE models [3-5] predict proportionality between γ

and electronic stopping power, dE/dx . But there are experimental studies where such a proportionality holds [6-8] and others where it fails [8-11]. It has been suggested by these authors that besides the direct interaction with target electrons, the incident ions also generate cascades of recoiling target atoms that may produce secondary electrons as well. The contribution of secondary electrons generated by recoiling target atoms to the total kinetic electron yield has not been unambiguously measured, which has crucial importance for complete understanding of the ion-induced electron emission phenomena. The objective of this experimental work was to test whether recoiling target atoms play some role in the secondary electron emission. For this purpose ion-induced secondary electron yields from ^{58}Ni and ^{60}Ni were measured. These targets have same electronic but different nuclear stopping powers, therefore any difference in the electron yield at a given ion energy will be most probably due to the difference of electrons generated by the recoiling target atoms.

2. Experimental Setup

The detailed description of experimental setup is given elsewhere [12]. Briefly the ions extracted

* Corresponding author : qayyum@pinstech.org.pk

from a duoplasmatron ion source were focused at the entrance aperture of $E \times B$ velocity filter by an Enzel lens. After charge and mass selection by $E \times B$ velocity filter, the ions were directed onto the 99.99 % pure polycrystalline ^{58}Ni or ^{60}Ni target that were placed inside a cage (see Fig. 1). The current density at the target surface was in the range of 40-95 $\mu\text{A}/\text{cm}^2$. The pressure in the target chamber was maintained at about 10^{-9} mbar by 400 l/s Varian ion pump. The target was mechanically polished, ultrasonically cleaned and placed perpendicular to the ion-beam direction. The target surface was kept dynamically clean with the ion-beam being used for the electron yield measurement. During initial cleaning process the surface condition was checked by measuring at intervals the electron yield and experiment was started after having a reasonably stable electron yield.

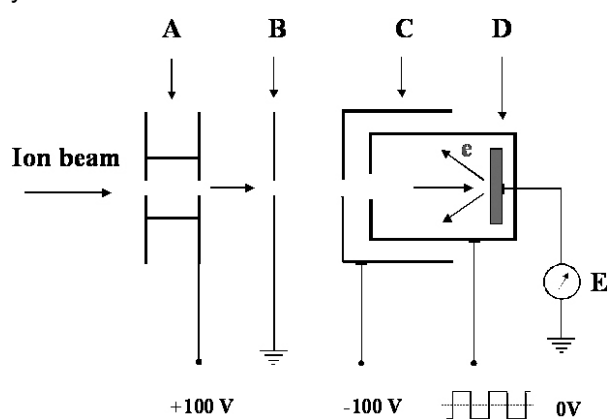


Figure 1. Schematic diagram of the experimental setup used for secondary electron emission studies. (A) Beam defining collimator, (B) Striping aperture, (C) rejection aperture, (D) cage and (E) Pico-Ampere meter.

Figure 1 shows the experimental setup for the measurement of secondary electron yield. A beam defining collimator serves to prevent the incoming ions from directly impacting the striping and rejection apertures and has a diameter of 2 mm. A potential of +100 V is applied to beam defining collimator to minimize ion-induced emission of electrons from its edges. The striping aperture prevents ions scattered by the collimator from entering the target region. The striping and rejection apertures have diameter of 3 and 3.5 mm respectively. A cage that is operated with a ± 80 V square wave generator surrounds the target in order to collect or suppress electrons emitted from

the target. The cage has an aperture of 4.5 mm for ion beam entrance, through which the incident ion beam collimated to 2 mm in diameter is able to reach the target surface. A rejection electrode at a potential of -100V was placed before the cage that prevents electrons from escaping and thus further enhances the electron collection efficiency. The current at the target is measured with a pico-ampere meter and then fed into a computer.

When applying + 80 V to the cage with respect to the target, the total current I_+ that is measured at the target consists of two components, the currents of incoming ions I_i and the current of emitted electrons I_e .

$$I_+ = I_i + I_e = I_i + \gamma(I_i/q) \quad (1)$$

Where q is the charge of incoming ion. For -80 V applied to the cage leads to a target current I_- that is equal to the incoming ion current

$$I_- = I_i \quad (2)$$

Therefore, the total electron yield is given as [13]

$$\gamma = \frac{I_e}{(I_i/q)} = q \frac{I_+ - I_-}{I_-} \quad (3)$$

3. Results and Discussion

The electron yield γ for normal impact of 2-10 keV Ar^+ on ^{58}Ni and ^{60}Ni targets is plotted versus ion energy in Fig. (2a). The indicated error bars show statistical error due to the current measurements. The following feature can be observed: (i) γ of both the targets increases with ion energy, and (ii) γ of ^{58}Ni is consistently higher than ^{60}Ni in whole ion energy range investigated here. The potential electron yield calculated using the semi empirical expression given by Kishinevskii [14] is equal to 0.075 electrons/ion which is same for both targets because potential electron emission depends on the work function of target material and the mean ionization energy of the incident ion. The KEE from metal targets has been extensively investigated theoretically [3-5]. As a main feature, the most frequently applied theoretical models consider kinetic electron yield γ to be proportional to the electronic stopping power D , that is

$$\gamma = \Lambda D \quad (4)$$

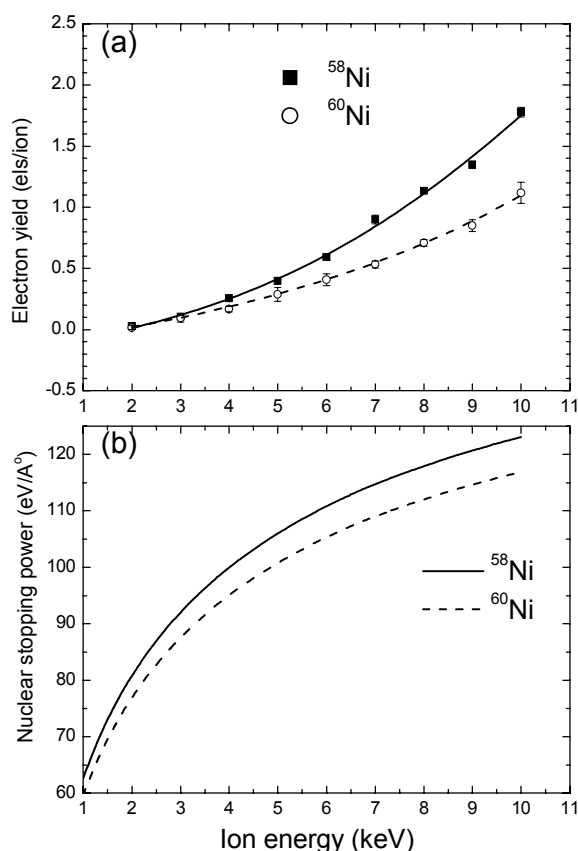


Figure 2. (a) The electron yields and (b) nuclear stopping powers as a function of Ar^+ energy for ^{58}Ni and ^{60}Ni targets.

Where Λ is a constant that depends on the material properties like the mean energy required for producing free electron within solid, the mean free path of electrons in solid and the escape probability of electrons to overcome the surface barrier. Consistent with the Eq. (4), γ of both the targets increases with ion energy. But the systematic difference in γ of ^{58}Ni and ^{60}Ni targets, which has same electronic stopping power for Ar^+ ions, is clearly not compatible with the Eq. (4). Previously, Eq. (4) has been roughly confirmed experimentally for ion bombardment of metals [6,7] and semiconductors [8]. The agreement between Eq. (4) and experiment is generally quite good for light ion bombardment. But for heavy ions, deviations from the simple rule given by Eq. (4) have been observed for several materials. For example Frischkorn and Groeneveld [9] for C^+ and O^+ impact on C, Jacobsson and Holmén [8] for Ar^+ , Kr^+ and Xe^+ impact on SiO_2 , Rothard et al. [10] for C^+ , and O^+ impact on Cu and Svensson et al. [11] for Ar^+ and Xe^+ impact on Al showed that kinetic

electron yield increase more slowly with D than predicted by Eq. (4). It has been suggested by these authors that for heavier projectile ions having keV energies, a sizeable contribution to electron emission is due to the energy deposited by the recoiling target atoms in the solid. Recently, Ohya [15,16] and Ullah et al. [17] has estimated yield of secondary electrons generated by recoiling target atoms for heavy ion impact on Al and MgO targets respectively using the Monte Carlo computer programs.

In the KEE models [3-5], the electron emission from material surface induced by the impact of energetic ions consists of the following three successive steps. (1) The generation of excited electrons in solid by kinetic energy deposited by the incoming ions. (2) the transport of these electrons towards the solid surface, and (3) finally the escape of electrons through the surface into vacuum. One can safely assume that mean free path of electron in the solid, kinetic energy distribution of electrons arriving at the surface and surface work function of both targets is same. Thus, the difference in γ we observed for ^{58}Ni and ^{60}Ni targets seem not to be related to step (2) and (3). Concerning step (1), at moderated and low projectile velocities the energy deposition profile of the projectile ion may be distorted drastically by the effect of nuclear scattering. As a result substantial electronic excitations can be due the energy deposition of recoiling target atoms. Therefore, for low velocity heavy ions the basic relation for kinetic electron yield has been modified as [4,11] :

$$\gamma = \Lambda (D_p + D_r) \quad (5)$$

Where D_p and D_r are the mean energy per unit depth deposited in electronic excitation by the primary ion and by the recoiling target atoms respectively. In Fig. (2b) nuclear stopping power calculated by computer code SRIM 2008 [18] is plotted as a function of projectile ion energy. By comparison of Fig. (2a) and (2b), one can extract following two similarities between the measured electron yields and the nuclear stopping powers. First, at a given projectile energy the nuclear stopping power as well as the electron yield of ^{58}Ni is greater than ^{60}Ni . Second, the difference in measured electron yield of ^{58}Ni and ^{60}Ni , and nuclear stopping power of ^{58}Ni and ^{60}Ni slowly increases with projectile energy. Next, the measured electron yield of ^{58}Ni and ^{60}Ni is plotted

as a function of the respective nuclear stopping power in Fig. 3. Considering the experimental uncertainties, the electron yields of ^{58}Ni and ^{60}Ni is almost same at any given value of nuclear stopping power. The matching of values and trends of the electron yields of ^{58}Ni and ^{60}Ni is indeed remarkable. Thus the higher electron yield of ^{58}Ni as compared to ^{60}Ni is due to the greater contribution, i.e. D_r , of the recoiling target atoms to the electron yield.

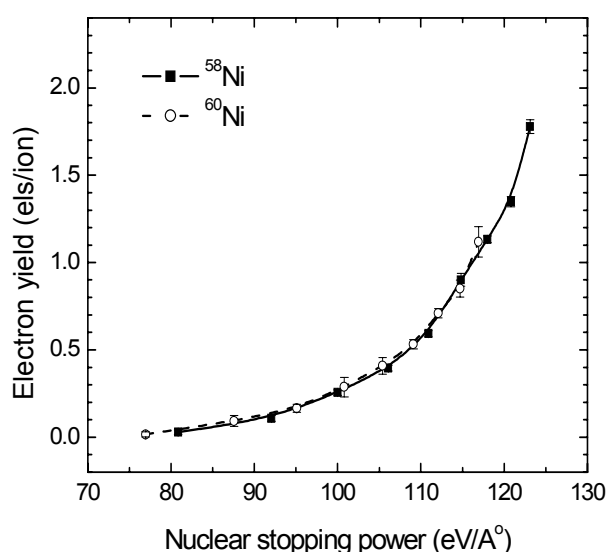


Figure 3. The electron yield as a function of nuclear stopping power for Ar^+ impact on ^{58}Ni and ^{60}Ni targets.

In summary, we have provided a clear evidence of secondary electrons generated by the recoiling target atoms. This indicates that, at least in this ion energy range, the proportionality between secondary electron yield and electronic stopping power does not exist. Further work on the measurement of secondary electron yield from metallic and insulator targets having same electronic but different nuclear stopping is in progress.

Acknowledgement

This work was partially supported by the Higher Education Commission of Pakistan through indigenous Ph.D program.

References

- [1] D. Hasselkamp, in: Particle Induced Electron Emission II, Eds. G. Höhler and E.A. Niekisch, Vol. 123, Springer, Heidelberg, 1992.
- [2] R.A. Baragiola, Nucl. Instr. Meth. B **78** (1993) 223.
- [3] E.J. Sternglass, Phys. Rev. **108** (1957) 1.
- [4] G. Holmén, B. Svensson, J. Schou and P. Sigmund, Phys. Rev. B **20** (1979) 2247.
- [5] J. Schou, Phys. Rev. B **22** (1980) 2141.
- [6] O. Benka, E. Steinbauer and P. Bauer, Nucl. Instr. Meth. B **90** (1994) 64.
- [7] H. Rothard, K. Kroneberger, E. Veje, A. Clouvas, P. Lorenzen, N. Keller, J. Kemmler, W. Meckbach and K.O. Groeneveld, Phys. Rev. A **41** (1990) 2521.
- [8] H. Jacobsson and G. Holmén, Phys. Rev. B **49** (1994) 1789.
- [9] H.J. Frischkorn and K.O. Groeneveld, Physica Scripta, T **6** (1983) 89.
- [10] H. Rothard, K. Kroneberger, M. Burkhard, J. Kemmler, P. Koschar, O. Heil, C. Biedermann, S. Lencinas, N. Keller, P. Lorenzen, D. Hofmann, A. Clouvas, K.O. Groeneveld and E. Veje, Radiation Effects and Defects in Solids, **109** (1989) 281.
- [11] B. Svensson and G. Holmén, J. Appl. Phys. **52** (1981) 6928.
- [12] A.H. Dogar, Shakir Ullah and A. Qayyum, Nucl. Instr. Meth. B **260** (2007) 525.
- [13] H. Eder, W. Messerschmidt, H.P. Winter and F. Aumayr, J. Appl. Phys., **87** (2000) 8198.
- [14] L.M. Kishinevskii, Radiat. Eff. **19** (1973) 23.
- [15] K. Ohya, Nucl. Instr. Meth. B **195** (2002) 281.
- [16] K. Ohya and T. Ishitani, Applied Surface Science, **237** (2002) 606.
- [17] S. Ullah, A.H. Dogar and A. Qayyum, Eur. Phys. J. Appl. Phys. **44** (2008) 235.
- [18] J.F. Ziegler, SRIM 2008, <http://www.srim.org/>.